QUEENSLAND UNIVERSITY OF TECHNOLOGY
COMMONWEALTH SCIENTIFIC AND INDUSTRIAL RESEARCH ORGANISATION

# Impact Detection on Spacecraft

EGH400 Honours Thesis Project



29th February 2021 – 19th November 2021

# Abstract

The topic of impact detection on spacecraft – specifically involving micrometeoroid impacts, dust, or debris – was explored. The research was motivated by the impact of the NASA Space Shuttle Columbia disaster on the global space industry, which highlighted the importance of embedded impact detection capabilities. A focussed review into the literature and current state-of-the-art highlighted three systems currently in use; of these, the project sought to provide a comprehensive replacement for NASA's micrometeoroid orbital debris damage recording system. The project aimed to generate a solution that was inexpensive, with design considerations for manufacturing and component selection; low power, indicative of an analogue solution; light weight and modular; maintainable and repairable, which would be aided by a modular approach; and flexible to apply to existing structures and technologies. The system was designed initially in MATLAB's Simulink, before conversion to a circuit model where it was tested in LTspice. Once verified, the system was designed in Altium Designer and ordered. The system was tested; results demonstrate full system behaviour that supports the model and simulation.


# Declaration of Conflicts of Interest

The author declares no conflicts of interest including competing financial interests. Funding for production was provided by the CSIRO. The QUT and the CSIRO were both involved as advising bodies.


# Acknowledgements

I would like to thank Professor Clinton Fookes, Associate Professor Luis Mejias Alvarez, and Dr. Jonathan Ralston for their assistance, inspiration, and support over the project period. Thank you to my roommate, Tina Behzadpour, who endured hearing about every detail, and who provided cups of tea in my late-night moments of need. The biggest thank you to my father, Dean Claxton, who tirelessly helped diagnose the final prototype. Without your expertise, the issues could not have been found and repaired.

# Contents

# 1.0.0 Introduction

## 1.1.0 Scope

This thesis explores the topic of impact detection on spacecraft, specifically involving micrometeoroid impacts, dust, or debris. The research is motivated by the impact of the NASA Space Shuttle Columbia disaster on the global space industry, which highlighted the importance of embedded impact detection capabilities. The thesis will commence with a focussed review of existing impact detection methods to understand the current state of the art. A lightweight detection system will then be designed and constructed based on readily available analogue electronic components. If time permitting, the prototype impact detector will be assessed through a practical experimentation in lab conditions to assess performance for detecting impact position. Future opportunities will also be explored for other space mission activity such as in-situ resource utilisation where monitoring impacts from debris remains an important and open problem.

## 1.2.0 Motivation

On the 1st of February 2003, the NASA spacecraft *Columbia* (Mission STS-107) was tragically lost along with the seven crewmembers [15]. The accident occurred due to a "catastrophic failure" resulting from a breach of the reinforced carbon panels on the underside of the left wing of the spacecraft. This breach was later traced to the lift-off stage of the mission, where a piece of falling foam from the external tank struck the panels [23]. The mission had been ongoing for seventeen days, with the crew unknowing of the incident in the first few minutes. In fact, *Columbia* was approximately fifteen minutes from touching down at the Kennedy Space Center (KSC) in Florida. This disaster, along with the loss of the spacecraft *Challenger* seventeen years prior, are the deadliest space accidents to date [08]. In hindsight, the accident was entirely preventable, given the crewmembers could have discovered the damage. Better yet would be if a system were inbuilt into the spacecraft that had detected the impact and alerted the crew instantaneously. The crew may have been able to abort the mission or perform maintenance in-orbit (or wait to be rescued).

Although in the case of the *Columbia* the impactor was material from the external fuel tank, a similar mission result could have occurred for any of the shuttle missions if an impact had occurred in orbit. Orbital debris is extensive from the last fifty years of spaceflight. It may be natural debris, but more than likely it is the result from previous missions or satellites as fragments [35]. Typically, the debris with a diameter between 1 mm and 10 cm are of most concern, as they fall within the category of being too hard to track from the surface whilst also being large enough to cause serious damage [35].

One significantly large fear for those concerned is the dreaded 1970's theory Kessler Effect/Syndrome (or sometimes referred to as collisional cascading), where a chain reaction of collisions could lead to an impenetrable barrier to space. If a critical mass of debris exists in orbit, a runaway reaction may occur where an orbit becomes highly populated with debris from the destruction of previous satellites [14]. Effectively, entire orbital paths can become impenetrable due to the inability to avoid high speed shrapnel clouds, which threaten to destroy inbound spacecraft; should a spacecraft fall victim, this would only worsen the situation. Consequently, there is a need (arguably external to the preservation of human life) for detection systems.

## 1.3.0 Client and Key Contributor Profiles

This project was put forward by the author to QUT, with the aim of contributing to the national space road map for Australia, which outlines goals across related sectors for the coming years. The CSIRO has joined the project to offer advice and guidance, especially as they are leading some of the efforts for research with their Space Technology Future Science Platform (FSP).

### 1.3.1 Organisations

The Commonwealth Scientific and Industrial Research Organisation (CSIRO) – Australia's national science agency - seeks to "solve the greatest challenges through innovative science and technology". Their business is defined by the Science and Industry Research Act 1949, which states they are to carry out scientific research and to encourage or facilitate the application or utilisation of the results of such research. Their research may be for any of the following purposes: to assist Australian industry; to further the interests of the Australian community; to contribute to the achievement of Australian national objectives or the performance of the national and international responsibilities of the Commonwealth; and for any other purpose determined by the Minister. [11][12][13]

The Queensland University of Technology (QUT), home to nearly 50,000 students, seeks to provide real-world skills to graduates. The university's research is extensive across many science and technology disciplines, with strengths in robotics, genomics, materials science, future enterprise, biomedical technologies, agriculture, and data science. Currently, QUT's efforts in space technologies and aerospace are largely housed under the Faculty of Engineering, within the School of Electrical Engineering and Robotics. [37][38][39]

### 1.3.2 Supervisors

Prof. Clinton Fookes is within the Signal Processing, Artificial Intelligence, and Vision Technologies (SAIVT) group at QUT. He is a Professor within the Faculty of Engineering, specifically in the School of Electrical Engineering and Robotics [19]. Prof. Fookes is the AI Theme Leader for the $250M SmartSat Cooperative Research Centre (CRC), which seeks to develop technology and skills for sectors such as advanced telecommunications and intelligent satellite systems [34].

Assoc. Prof. Luis Mejias Alvarez has been the Deputy Director for the Australian Research Centre (ARC) for Aerospace Automation, as well as the Chair for the Queensland IEEE Control Systems Society and the Robotics and Automation Society. He is an Associate Professor within the Faculty of Engineering, specifically in the School of Electrical Engineering and Robotics. His work has included research into unmanned aerial systems (UASs) including computer vision and emergency landing systems. [04]

Dr. Jonathon Ralston, a Senior Principal Research Scientist who is currently leading the integrated mining research at the CSIRO, has joined the project as the CSIRO supervisor. His expertise and work within the CSIRO spans nearly 25 years, and his fields of research include control systems; robotics and automation; guidance, navigation, and control; and remote mining technology. Dr. Ralston is leading new activities for developing niche capability within the Space Technology FSP with a focus on in-situ research utilisation (ISRU). Due to the nature of the research pertaining to this project, the goals align strongly with the aims of CSIRO's Space Technology FSP. [27]

## 1.4.0 Relevancy

Established in July 2018, the Australian Space Agency (ASA) is a relatively new organisation founded to coordinate and support the growth and transformation of Australia's space industry [05]. The 2019-2028 Australian Civil Space Strategy (ACSS) outlines several national civil space priorities, including position, navigation, and timing; Earth observation; communications technologies and services; leapfrog research and development; robotics and automation on Earth and in space; access to space; and most importantly for this project, space situational awareness and debris monitoring [06].

The ACSS mentions the CSIRO in funding and collaborative missions, as they are one of the major organisations supporting its development and on-going activities [06]. The Space Technology FSP collaborates with the National Aeronautical Space Administration (NASA) in the United States of America, and other large organisations, which draws attention back to Australia and highlights the desire to contribute. For the work within ISRU, this is the CSIRO showing their capabilities by targeting niche technologies, which will have a significant contribution to the current space race to Mars. This is the same driving motivation that is behind SmartSat CRC. Funded by the Australia Government [34], they are a component of the Australian Government's plan to promote innovation and technological development in the space field. The project work will largely focus on aspects that will complement the Space Technology FSP in developing niche technologies.

For the audience that the author represents, this project represents an effort to highlight the interest and desire for study components, research, and projects relevant to the space industry. Hence, this project has a motive for a social impact: to connect industry such as the CSIRO with academics at QUT to promote this effort. The project also aims to have an economic impact by contributing to technology that will enable safer missions, minimise losses and therefore expenses, and reduce time spent on manual inspections. Over the next ten years, as outlined by the ACSS, the Australian space industry is expected to grow significantly. This project hopes to contribute to the development of technology.

## 1.5.0 Considerations

The project has several explicit and implicit constraints. As it is a student undergraduate project, it cannot be anything too immense or intensive; the product must be reasonable, especially as there are time constraints. Effectively there are 26 weeks (split into two semesters of 13 weeks, with a five-week break period in the middle) for work to be performed. Note that there are also mid semester breaks and exam block periods; in full, from start to finish, is a length of 36 weeks.

Given the global pandemic, this project will be living in the shadow of COVID19. Current Australian government strategies include snap lockdowns, which may disrupt the project or communication between involved parties. Manufacturers may be operating slower than usual, there may be delays, or required components may be unavailable whether that is temporarily or permanently. To compensate and to ensure readiness for sudden situational changes, communication with involved parties should be on virtual formats or with a virtual format readied. If parties are meeting in person, then social distancing procedures will be followed.

Although QUT and the CSIRO are on-board as advisors and supervisors, they are not financial sponsors for the project. Monies for expenses must be covered by the student unless in exceptional cases. Consequently, prototypes and products constructed will be cheap, inexpensive, and making full use of student facilities such as the S-Block labs and O-Block LaunchPad.

### 1.6.0 Fields of Consideration

The title of this project, "Impact Detection on Spacecraft", offers a wide variety of interpretation to the direction of the project. The term *spacecraft* alone suggests several concepts and ideas, such as satellites, space stations, surface vehicles, ascent vehicles, rovers, space bases, and many more, which may have been overlooked. Furthermore, impact detection can be broken down into several "groups", depending on definition or method.

When focussing on detection (assuming the project is to develop some form of sensor technology), there are several types, which need to be considered. These offer extreme adjustments to the project scope. If the sensor is to detect whether an impact has occurred, this may involve recording vibrational, mechanical, thermal, or pressure changes to the body. Again, each of these alone may offer extensive opportunities for research. Moving away from whether an impact has occurred, alternatives may include whether an impact is imminent, determining whether nearby objects are threats for a potential impact, or a simple proximity alert system. The commonality here is the desire for some form of alert system, with the flexibility to select the condition of impact for which the user should be alerted.

Similarly, the impactor is undetermined. The project may focus on gaseous or ionic particles, which may be unthreatening unless travelling at relativistic speeds. On the other end of the spectrum, perhaps the user is interested in terrain contact, which could include navigating an asteroid or landing on a planetary surface. A user may also be interested in other spacecraft, which bares similarity to the previous example, as there are two key purposes. Primarily, this would be the detection of unplanned or undesirable impact events, whether that is with terrain or another spacecraft. Otherwise, the detection of desired impact events, which may include touchdown on a surface or the successful connection of space station modules. Two other broad categories can be discussed, which would include debris (from potential sources such as dysfunctional, destroyed, or decommissioned spacecraft) and micrometeoroids. The latter is frequently referred to as micrometeoroid orbital debris (MMOD). These categories suggest that the project needs to specify some sort of size target, whether that is some level of microscope or macroscopic. Additionally, it may be worth specifying the environment as the factors for consideration vary wildly when considering orbital, suborbital, or surface conditions.

As can be seen in the fields of consideration, the project scope can have considerable breadth. To narrow the field, this project will be focussing on detecting impacts that have occurred, and with a focus on sensing MMOD strikes. By considering some simple scientific concepts in the context of the problem, this drastic reduction of project scope still offers a significant challenge. If the aim is to develop some form of alerting system that could be deployed onto an existing or to-be-manufactured space vehicle, the project needs to recognise the complexity of the construction processes of these space vehicles. The device, sensor, material, or result of the project – from here on referred to as the product or project product – must either be able to survive the harsh conditions of space or be deployable within the protective "skin" of the spacecraft. If the former, this may include thermal factors (regulation or re-entry considerations), radiation or high-energy particles (especially regarding electronics), or vacuum (or near-vacuum) environments. If the latter, then detection may face issues with either interference, artefacts, or attenuation of signals depending on the method.

## 2.0.0 Literature Review of Existing Technologies

Existing technology is quite diverse and continues to develop, as there is a need to design a system, which can replace the Wing Leading Edge (WLE) Impact Detection System (IDS). The WLE IDS is a delicate and vulnerable system and does not operate during the entire mission due to power consumption [35]. It consists of accelerometer sensors, which sample at 20 kHz. Typically, it only functions during mission launch [35]. This is due to battery power as only ten hours of monitoring, depending on temperature, is available [10]. WLE IDS must be accompanied by optical inspection, which is an arduous process [35].

## 2.1.0 MMOD Damage Recording System

Prompted by the *Columbia* accident, the MMOD Damage Recording System (DRS) was integrated into the Thermal Protection System (TPS) of the shuttles [35]. MMOD DRS was designed for usage throughout a mission's entirety. It consists of a series of nodes, where each node contains up to eight Embedded Damage Recorders (EDRs), a Wireless Data Acquisition System (WDAS), and up to three shock micro sensors. The system has been designed for deployment to vulnerable structures or key points of interest [35]. The EDRs consist of a network of traces, which can be used to determine a region of minimum or maximum damage to the structure (Figure 2.1.0A).

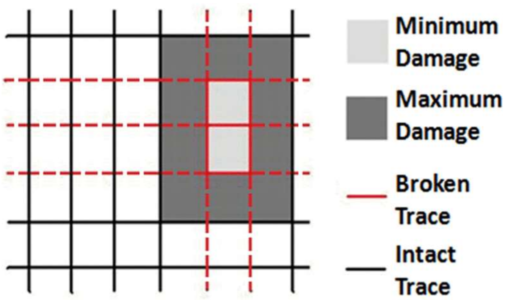


Figure 2.1.0A: Example EDR case, where damage has broken five traces. The impact position can be roughly located [23].

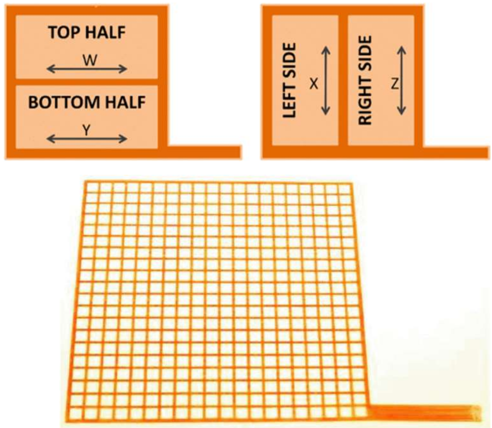


Figure 2.1.0B: Layering of the axes (upper diagrams) results in a square grid sensor (lower diagram) [23].

This is accomplished by a two-layer grid of traces where each layer consists of traces running on perpendicular axes. When layered correctly, a square grid is formed (Figure 2.1.0B). The assemblage is produced on a flexible material using copper traces and is referred to as a "Serpentine EDR Sensor" [35]. This is then integrated into the thermal protection system (TPS) stack as a single layer. The grid is routinely checked by the WDAS via voltage inspections on each trace. It can be interrupted by an impact event as detected by the shock micro sensor, which forces an inspection. On completion of each inspection, the WDAS transmits relevant information to the on-board health monitoring system to be interpreted by flight crew when/where necessary.

## 2.2.0 Distributed Impact Detection System

The Distributed Impact Detection System (DIDS) uses Acoustic Emission (AE) techniques for monitoring structural health [10]. The general concept involves the detection of structural waves using piezoelectric sensors, accelerometers, and AE sensors built into a standalone device (Figure 2.2.0A). The device can be installed anywhere on a structure; it may be collocated for a higher degree of accuracy. Each device has four channels which allows for "…reliable triggering and subsequent [triangularisation]" [10]. This is performed using relative Time of Arrival (TOA) information.

The specifications intend for a quiescent current of less than 30 µA and a 2 µs response time. Unlike the MMOD DRS, data must be acquired

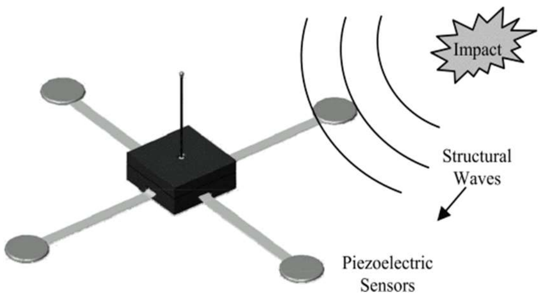


Figure 2.2.0A: DIDS System Concept [07]

during the incident. The DIDS system has been tested on-board the international space station (ISS) and on sub-orbital rocket launches. When recovered from a crash, no faults or failures had occurred and a complete data set was downloaded, which listed all (275) recorded events. These corresponded to mission preparation, launch, and eventual crash [26].

## 2.3.0 Fibre Bragg Grating Sensor System

As fibre-optics technology develops, equivalent sensors continue to be produced – although at higher cost – with advantages in sensitivity, passivity, electromagnetic interference (EMI) immunity, and form factor; this has included applications from vibration, magnetic fields, temperature, viscosity, and various other traditional sensors [09].

Fibre Bragg Gratings (FBGs) are an application of fibre-optics for the detection of strain. The core structure of an FBG is a short piece of optical fibre, which has been designed with a specific internal reflection pattern (Figure 2.3.0A).

The result is an ultra-specific wavelength pattern that is emitted after electromagnetic radiation (EMR) traverses the FBG (Figure 2.3.0B). By consequence, any change in length will change the output. Due to the wavelength of EMR used (typically in the ultraviolet (UV) range), the sensor is extremely sensitive to change.

Figure 2.3.0A: FBG strain-sensor-tube example [02]

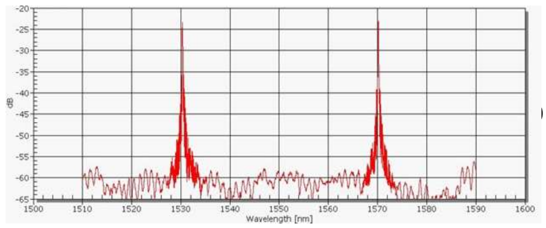

Figure 2.3.0B: FBG strain sensor output peaks, which allows for the determination of the wavelength and therefore the change due to strain. [02]

Generally, the relationship for the strain from the wavelength can written as:

Where $\varepsilon$ is the strain, $L$ is the initial length, $\lambda$ is the [41] wavelength, $\Delta L$ and $\Delta\lambda$ are the changes in the respective lengths and wavelengths, and $k$ is some scalar that changes depending on the specific FBG used; for a conventional single mode fibre SMF28 this is approximately 1.27 [09]. This relationship is the key component of FBGs; this application of fibre-optics in sensors is known as the index modulation geometry [09].

## 2.4.0 Literature Discussion

The three systems reviewed approach the issue from different angles, and each has advantages and disadvantages.

The MMOD DRS is a cost-efficient method of determining where damage has occurred. The system can be implemented directly into the TPS stack as a single layer. If done correctly, it will provide a permanent record of damage across the entire spacecraft. This record contains a minimum and maximum region of damage for each impact site. Issues however include analysis of the traces when spacecraft-wide, and potential false negatives depending on impact position and trace grid dimensions.

The DIDS can determine position of impact and force. When collocated, accuracy and detection capabilities increase. The system is more complex than the MMOD DRS and does not create a permanent record (other than in software) as it listens for transient behaviour in AE. The system is arguably more vulnerable, yet easier to repair and maintain due to its modular nature. As the system involves piezoelectric- and other AE sensors, DIDS is more expensive than MMOD DRS. DIDS is already at a high level of technology readiness due to rigorous testing and development through involvement with NASA.

FBGs are the latest development in applicable detection technologies. Due to their construction process and involved fibre-optics, they are considerably more expensive. Similarly (to the DIDS), they can be positioned in various locations over a structure. Unlike DIDS, they have not been thoroughly tested and have a low technology readiness level. Initial testing in controlled environments show high levels of accuracy and sensitivity, although the impacts were well in proximity of one if not multiple FBG sensors.

Given the constraints and nature of the project, investigating improvements or the application of the DIDS or FBG systems would not be feasible. This is largely due to cost, access to materials, and time constraints. The DIDS is highly developed, and so it would be unlikely that construction of an analogue device as well as an investigation would be feasible within the project timeline. Although this is not the case for the FBG system, fibre-optics would require specialty equipment and expertise that would not be available to the student.

The MMOD DRS offers the most promise for a student project. A prototype can easily be assembled from materials accessible by the student. As mentioned, shortcomings of the design include trace analysis and false negatives. This offers two areas of research that are current gaps in the literature.

# 3.0.0 Ideation & Design Development

With the delivery of the thesis proposal, Stage 1 has been completed. Stage 2 will pursue focussed research and design ideation. Upon investigation of the literature, the MMOD DRS system was pursued as the initial source of inspiration. One of the critical design shortcomings is the possibility of false negatives depending on the trace separation. Additionally, there is the possibility that an impact might only be traced to one axis if both longitudinal and latitudinal traces are not broken. Although this would still register an impact, the position would not be completely known. Depending on the size of the grid, this could be frustrating for maintenance and repair.

There are also concerns with applying the design to a large area. Many of these grids could be used and paired together, which likely would require some wired/wireless connection between many microcontrollers, or the grid itself is extended to cover the entire vessel. Both these applications do not seem practical. The former requires a considerable amount of power for running many microcontrollers, and the latter requires either large grid spacing, thus rendering the system redundant, or extreme finesse and technical planning to ensure the traces remain connected, wired correctly, and maintain the maximum separation distance across the structure.

Given these factors, and the wider scope of understanding of the project, several constraints – in addition to project considerations – have been formed:

**Prototype**: The project should be able to produce some form of prototype system for presentation and testing. This may include hardware and software components.

**Component Selection**: The product should be as inexpensive as possible. This is to conform to both project considerations and industry interest.

**Target Destination**: The product is to be designed as a precursor to a system that could be used on spacecraft. This means that component selection and system design should include this. Aspects such as weight and size are significant. Furthermore, components that are radiation-hardened (or would have radiation-hardened alternatives) are desirable.

**Competitive**: The minimisation of use of microcontrollers will drastically reduce the price, as these would ordinarily be extremely expensive as radiation-hardened alternatives. Furthermore, power consumption is a strong concern. The use of passive components, low-power electronics, and analogue techniques will be necessary to produce a cost-competitive product.

**Implementation**: An advantageous factor to any design would be its ability for rollout on existing systems, and eased integration into future designs.

**Maintenance and Longevity**: The product should be repairable and maintainable if it were to be used on long-duration spacecraft. This may include modularity for switching damaged components.

### 3.1.0 Initial Design Concept

To summarise the research and discussion thus far, the designed solution should be inexpensive, with design considerations for manufacturing and component selection; low power, indicative of an analogue solution; light weight and modular; maintainable and repairable, which would be aided by a modular approach; and flexible to apply to existing structures and technologies. Therefore, a system with layers of control and a tree-like hierarchy would be a suitable system architecture, as this would enable both flexibility and modularity.

Consider the MMOD DRS system mentioned in literature: this design embeds damage history of a region by examining broken traces; however, each location requires two signals that are mapped backwards to determine impact location. Although little information on how this solution would be applied to provide detection capability to entire structure, it can be assumed, each module would link together with an information feed interpreted by some controlling processor (likely the mentioned WDAS). To arrive at the new design, the MMOD DRS limitations will be examined.

Consider the methodology of impact detection in the MMOD DRS, as indicated in the literature in Figures 2.1.0A and 2.1.0B. Both false negative detections (an impact that causes mechanical damage without registering, which would be in the case no trace is broken) and partial detections (an impact that causes mechanical damage and breaks a singular trace, which is insufficient information to determine the location) are possible. By nature of the system, the traces should run parallel and perpendicular to each other to ensure consistency in detection capability and to eliminate the risk of false negative or partial detections. This places several restrictions on layout and consequentially generates issues for applying the design to curved surfaces. Consider instead a plate-based system, where damage can be identified by singular plate failure. When compared to the MMOD DRS, the new technique has a 1:1 mapping for signal connections (traces) to plates, compared to the 1:2 mapping for the MMOD DRS; this has been visualised in Figure 3.1.0A.

When considering the traces of the MMOD DRS in Figure 3.1.0A, non-uniform surfaces (represented by the warping of the second mesh) would create regions of inconsistency in separation distances. This is critical when considering that the separation distances translate directly to the resolution of the system's detection capability. If instead a plate-based

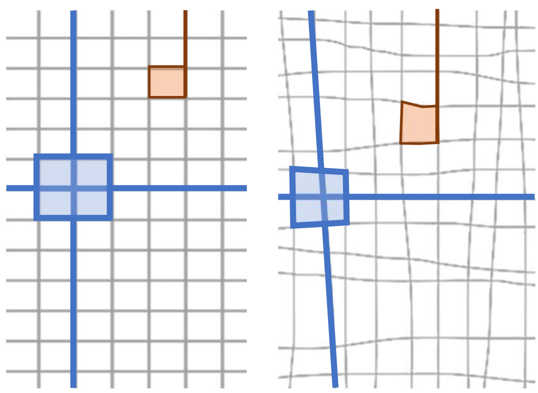

Figure 3.1.0A: Comparison of detection techniques with simple (left) and complex (right) surfaces. Blue lines represent the MMOD DRS traces, with the highlighted region as the example the detection zones. Orange represents the new scheme, with a single signal (with return) for each plate.

## 3.2.0 Logical Model Design

To help progress the design, the theoretical model was assembled in MATLAB's Simulink environment. Three tile groups were assembled and simulated. As seen in Figure 3.2.0A (right pane), each tile group was configured to have two inputs. One input was common and is connected directly to the computer's sinusoidal signal generator shown within the computer masked block, Figure 3.2.0A (left pane). The other input was a simulated damage matrix, which was generated in a MATLAB script (Appendix A) when running the simulation environment.

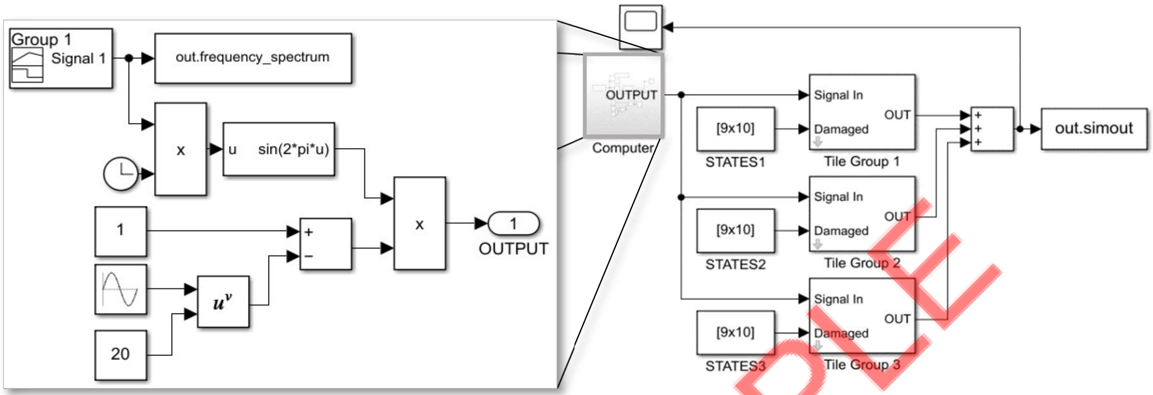


Figure 3.2.0A: High-level overview of the logic model, as constructed in MATLAB's Simulink environment.

The tile group subsystem was implemented as a masked block, with parameters for damaged and tile identifier. This was to assist with configuration and scaling the model. The lower-level blocks, such as the tiles as seen in Figure 3.2.0B, have an input for their identifier. This was to assist in revisions for the model; re-entering tile identifiers when updating tiles with the latest version was an arduous and needless exercise. The damage matrix fed down from the highest level is split by row before entering each tile. Figure 3.2.0B shows the damage matrix transforming into nine different outputs, which correspond to each row. It should be noted that the sinusoidal signal does not flow into the tiles and is handled completely separately as described in the Initial Design Concept Discussion. Note that a 28$^{th}$ order Butterworth band-pass filter was used to model the filter attenuation. The outputs of the tile groups are summed together with the new period indicator, which is generated from a pulse function and multiplied by a gain term.

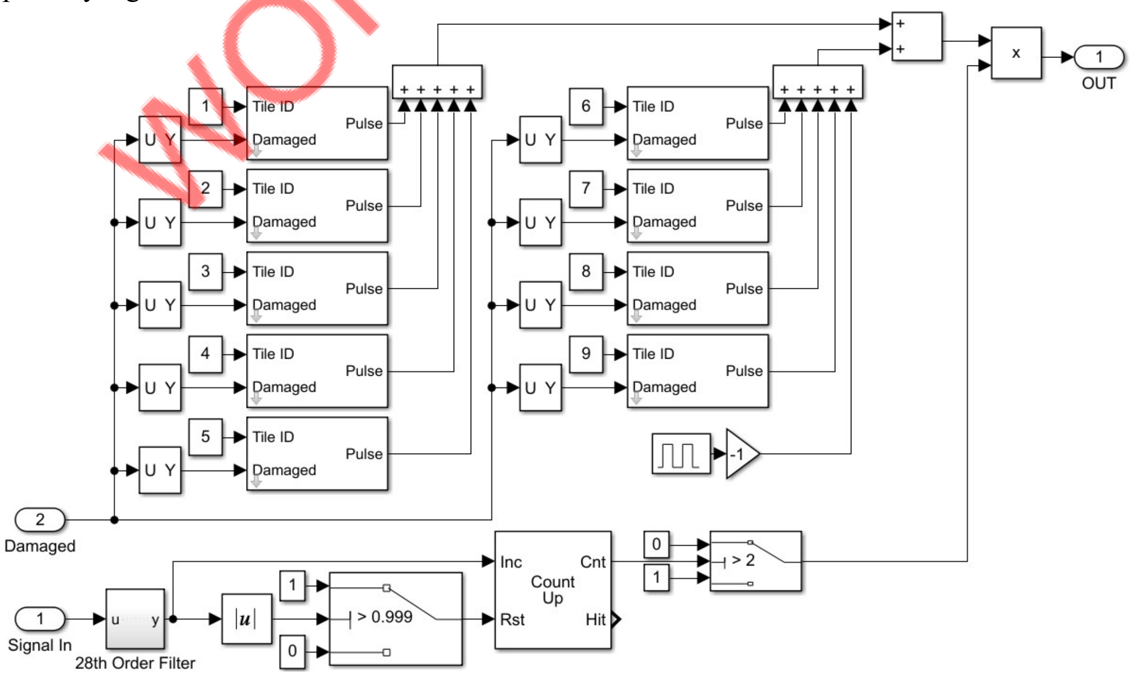


Figure 3.2.0B: Overview of the Tile Group subsystem.

## 3.3.0 Simulating the Logic Model

To test the behaviour, the damage matrices were randomised, and the input sinusoidal signal was varied. The overall results are shown below in Figure 3.3.0A. During the simulation, the signal alternated between holding a frequency for 0.2 seconds, or linearly increasing to the next frequency (except for the initial held frequency of 0 Hz, after which the signal jumps to 90 Hz to commence linearly increasing). The frequencies that were held were 0 Hz, 101 Hz, 102 Hz, 103 Hz, and 114 Hz. This variation can be seen on the secondary axis in the first plot pane of Figure 3.3.0A. The final frequency was arbitrarily selected to help eliminate transient behaviour and distance the signal from any of the natural frequencies of the tile groups. A starting frequency of 0 Hz was selected to help minimise start-up noise whilst simulating a likely system initial condition. The frequencies 101 Hz, 102 Hz, and 103 Hz corresponded to the natural frequencies of the three tile groups as seen in Figure 3.2.0A. Due to some transient behaviour, it can be seen in Figure 3.3.0A that there was some start-up system noise, as well as noise on the settling periods at the beginning of each held period (as the tile group does not relay information for the entire 0.2 seconds of hold time). This unideal behaviour is related to the filter design and can be improved or eliminated with more care in filter selection and staging.

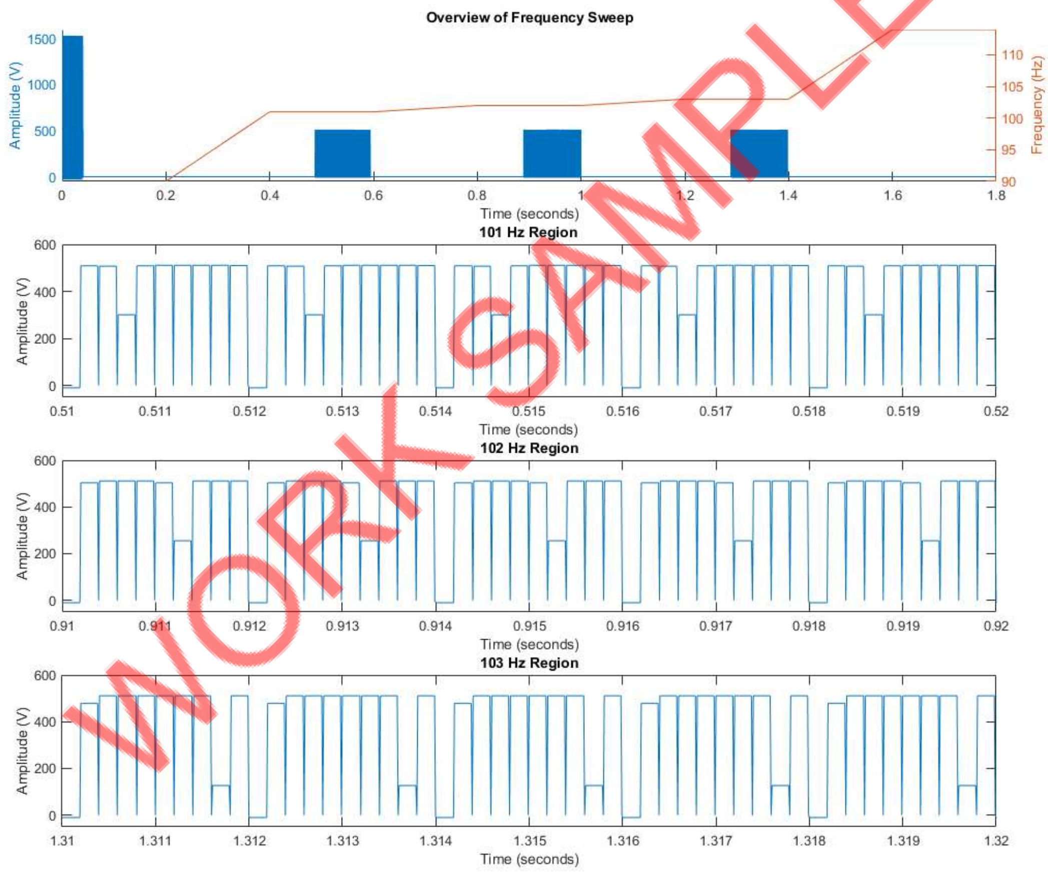


Figure 3.3.0A: Simulation results. The first plot pane depicts the overall behaviour of the system. The second, third, and last plot panes depict a truncated view of the upper plot pane.

Upon inspection of the second, third, and the last plot panes in Figure 3.3.0A, three unique pulse trains are evident. These were cross-referenced to the randomised input damage matrices and shown to be as expected. This is sufficient confirmation for the design to continue into circuit design.

# 4.0.0 Circuit Model Design

With a functional design, simulation can transition from MATLAB's Simulink environment into LTspice, where more complex circuit behaviour can be modelled. This process was done by considering mathematical functions, and then finding circuit blocks which can perform that function. The blocks can then be connected via buffers.

Consider the entire system, which can be broken into six building block types: the power system; the computer and interface; the tile group block, which will contain some number of tiles; the tile blocks, which will contain some number of plate set blocks; the plate set blocks, which will contain some number of plates; and the plates themselves. This has been visualised in Figure 4.0.0A, with two key topological differences present between this model of the system and that which was implemented in Simulink:

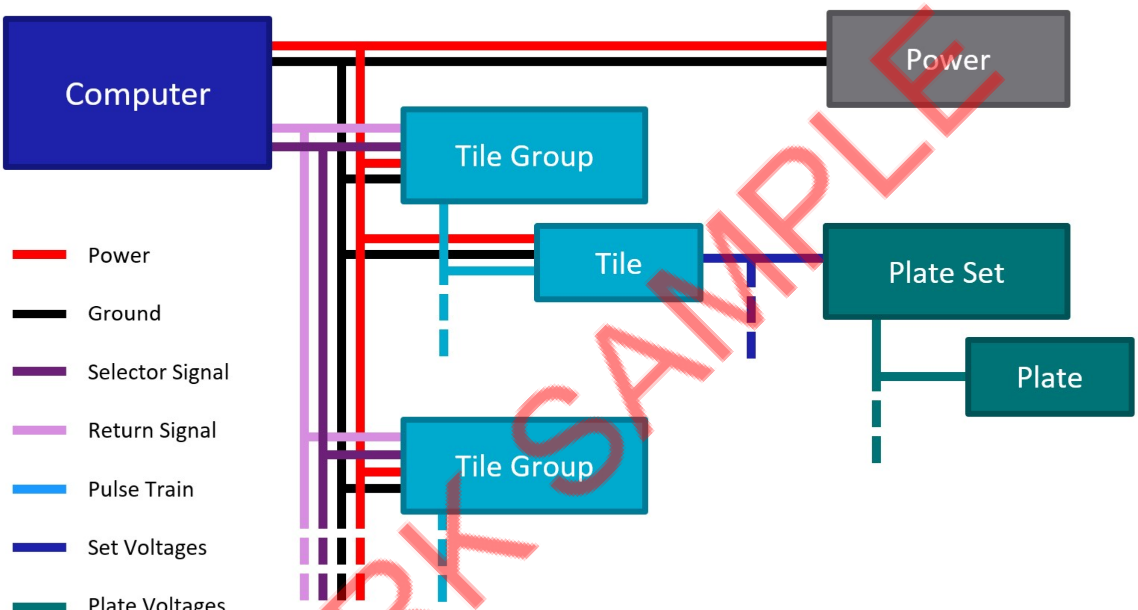


Figure 4.0.0A: Circuit architecture to be implemented. Return path is controlled by a selector signal; tuning frequency to match filter thresholds of specific tile groups. Internal to each tile group, the signal that is returned when requested is constructed as a pulse train, with tile information encoded in the time domain. Each tile corresponds to a collection of pulses, which are scaled according to plate set health (summative health of subset plates). Plate voltages sum as a tuned inverse proportional relationship.



Firstly, plates are assembled into plate sets prior to tiles. This necessary change compensates for the new relationships introduced as the model transitions into real electronic components. Unlike the direct proportional relationship described by the logic model, resistance sums as an inverse proportional relationship; the plate sets handle the tuning required. The encoding of tile information was previously as singular pulses. In the time domain, a tile now exists as a collection of pulses that are the individually scaled amplitudes of its internal plate sets.

Secondly, assemblies have been resized from base three (nines) to base two (fours). This assists in circuit design as many integrated circuits are pre-packaged in sizes that are base two (typically two, four, or eight). This also will drastically reduce the system requirements for signal analysis, as four plates in a plate set corresponds to sixteen voltage levels instead of the 511 previously required; a sixteenth of a 3.3 V source is around 0.2 V, compared to 6 mV for a 511$^{th}$. A larger voltage division from fewer voltage levels is preferred as it reduces the ADC specification minimums as well as robustness to noise.

## 4.1.0 Model Construction

Due to the number of components and system size, the project rescoped the product from a full system to investigating the feasibility of a single tile group. The control interface and overall system architecture in comparison is relatively simple and can be attempted at a future date. A tile group was assembled in LTspice and tuned to reduce noise. This latter step involved adjusting components, primarily the operational amplifiers and comparators used. After much experimentation, all comparators were replaced with operational amplifier chips in a comparator topology. The operational amplifier integrated circuit selected was the OPA353; due to the quantity required, the OPA4353 package (quad) was utilised – this is not evident in the LTspice as, by nature of the software, real circuit layout and printed circuit board (PCB) design is not considered.

When simulating the circuit under normal conditions, due to the computational complexity, only forty nanoseconds were required as this was sufficient data to view a whole tile time domain response. Data was recorded from the fifth nanosecond using the transient simulation command with "Skip initial operating point solution" enabled (this can be seen as the Spice Command in Figure 4.1.0A). When simulating the entire tile group, typically 400 nanoseconds were recorded starting from the 50th nanosecond. Bypass capacitors were not included in the LTspice model.



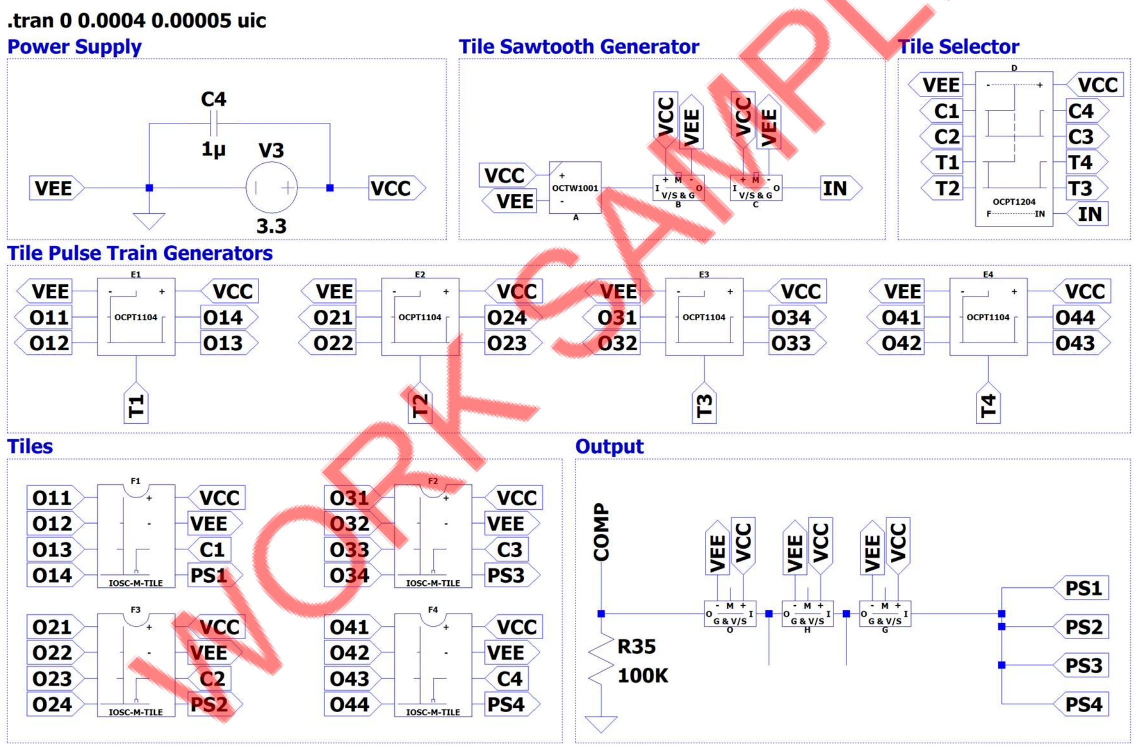


Figure 4.1.0A: LTspice overall model of the system. A single 3.3 V power supply is used. The Tile Sawtooth Generator translates to module (a) in Figure 4.0.4. Module (b) of Figure 4.0.4 is shown as the Tile Selector. The Tile Pulse Train Generators translate to module (a) and (b) of Figure 4.0.3A. Modules (d) and (e) of Figure 4.0.4 are contained within Output, which consists of three blocks; each block performs a subtraction and multiplication operation that apply an offset and gain respectively. The initial inputs into the Output block (PS1-PS4) enter in the range of 30 - 90 mV. The offset and gain operations scale the output to vary between 0.3 - 3 V.

Limitations of the model relate specifically to the ICs used. The TMUX1101 chip (a voltage-controlled analogue switch) had no spice model available, and so a representation was constructed from the dataset information available. Although a spice model was available for the operational amplifier IC, there may still be some deviation with real components particularly as the bypass capacitors were not modelled. Otherwise, general noise and other factors ignored relating to traces, vias, and component placement may skew the real behaviour. Component schematics are included in Appendix B. Simulation output is measured at COMP (Output).

## 4.2.0 Model Behaviour

The full system was simulated, and the output data downloaded into a text file. This was loaded into MATLAB for analysis. Figure 4.2.0A examines the simulation output at the COMP net (Output).

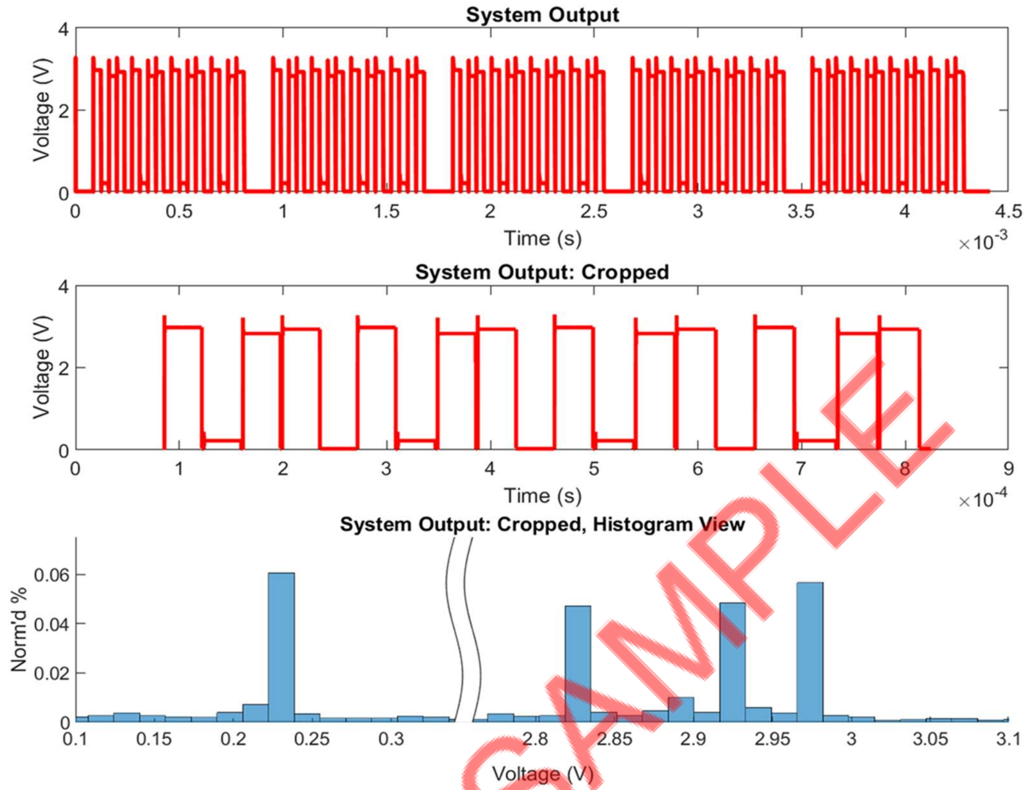


Figure 4.2.0A: Examination of system output over a simulation period of four milliseconds (top). When enlarged, the anticipated damage is evident in the variation in plate set pulse heights (middle). By further inspection, the four unique states are immediately obvious in the histogram representation (bottom).



For the results displayed in Figure 4.2.0A, all four tiles simulated have identical plate set health. To visualise a full spectrum of pulse amplitudes the highest, lowest, and two intermediate combinations were chosen. If the circuit is functioning correctly, a simple mathematical operation should yield the initial conditions. As can be seen by the histogram, the combinations approximately correspond to voltages in the regions (bins) of 2.97 $\pm$ 0.02 V, 2.93 $\pm$ 0.02 V, 2.83 $\pm$ 0.02 V, and 0.23 $\pm$ 0.02 V (in order of highest to lowest amplitude). Therefore, if these thresholds are A, B, C, and D respectively, then A corresponds to the lowest resistance (highest voltage) combination, and D corresponds to the highest resistance (lowest voltage) combination. By Table 4.0.2A, A must be combination 1 and D must be combination 16. To determine the remaining combinations, recall each voltage threshold for each combination is linearly dispersed between the highest and lowest. Therefore, as the difference is 2.74 V $\pm$ 0.04 V, each threshold is separated by 0.198 $\pm$ 0.003 V. This is sufficient information to convert from voltage level to combination, as the following formula can be used:

$$C_N = 16 - round\left(\frac{V_N - V_L}{S}, 0\right)$$

Where the combination $C_N$ can be solved for using the voltage threshold $V_N$, the lowest voltage threshold $V_L$, and the threshold separation $S = V_H - V_L$ (where $V_H$ is the highest voltage threshold).

$$C_B = 16 - round\left(\frac{2.93 - 0.23}{0.198}\right) + 1 = 16 - round(13.63) = 16 - 14 = 2$$

$$C_C = 16 - round\left(\frac{2.83 - 0.23}{0.198}\right) + 1 = 16 - round(13.13) = 16 - 13 = 3$$

By inspection of the cropped system output (Figure 4.2.0A, middle), it can be seen the heights are in the order of A, D, C, B. Therefore, the estimated combinations correspond to:

Plate Set 1: [1, 1, 1, 1] (Combination 1)
Plate Set 2: [0, 0, 0, 0] (Combination 16)
Plate Set 3: [1, 1, 0, 1] (Combination 3)
Plate Set 4: [1, 1, 1, 0] (Combination 2)

From LTspice, the keycodes entered for each tile were (SXX: State **PSI**, **PID**):

S11 = 1, S12 = 1, S13 = 1, S14 = 1
S21 = 0, S22 = 0, S23 = 0, S24 = 0
S31 = 1, S32 = 1, S33 = 0, S34 = 1
S41 = 1, S42 = 1, S43 = 1, S44 = 0

These correspond to:

Plate Set 1: [1, 1, 1, 1] (Combination 1)
Plate Set 2: [0, 0, 0, 0] (Combination 16)
Plate Set 3: [1, 1, 0, 1] (Combination 3)
Plate Set 4: [1, 1, 1, 0] (Combination 2)

As is evident, the model behaves as expected and the correct combinations could be estimated. The accuracy and speed would be greatly enhanced by an ADC and processor with the functions coded. Further testing yielded the same results. Therefore, circuit construction can proceed.



This space has been intentionally left blank.

# 5.0.0 System Production

For manufacturing, values were tuned to appropriate E12 series. Where possible, some components were replaced with multiples of 1 kΩ or 10 kΩ – for example, a 19.75 kΩ was replaced with two 10 kΩ resistors in series. Altium Design (AD) was used to design the PCB; one tile group was constructed on a singular board to ease assembly. Digi-Key was used as the primary collection of component datasheets, footprints, and 3D models. All resistor tolerances – other than the 1 kΩ and 10 kΩ resistors, which required 0.1% - were 1%. Bypass capacitors were selected with tolerances of 10%; a timing capacitor inbuilt into the sawtooth generators had a tolerance of 1%.

## 5.1.0 Fabrication Issues

To reconstruct the circuit in AD, LTspice schematics were compared side-by-side. Although this is not a perfect system, it succeeded in reducing the probability of copy errors. Originally, the LTspice schematics were composed with all operational amplifiers separated individually. This complicated the reconstruction, as in Altium the operational amplifiers were grouped as per their IC. Despite the best attempts, several errors were later identified. These range in severity:

1. Silk screen placement: Two sets of silkscreen identifiers overlapped, which obscured resistor labels. Digital circuit diagrams provided the missing information.
2. Reflow Error: A thermocouple moved during the reflow process, which caused a large temperature gradient to form across the PCB. This melted (destroyed) many of the physical SPST switches, which had to be replaced; test switches have been mounted, new parts are pending.
3. Component purchase
    a. An error in the bill of materials resulted in the TMUX1102 parts link appearing next to the TMUX1101 specifications. Unfortunately, the TMUX1102s were ordered and installed. The TMUX1102 is the logical not case of the TMUX1101; when the TMUX1101 is high, the TMUX1102 is low. To correct this in the absence of replacement parts, a transistor and resistor pairing was used at each selector pin for each TMUX1102 installation, which performs another logical NOT to invert the input signal thus correcting the output. This correction resolves the issue however introduces significant amounts of noise. TMUX1101 parts are pending.
    b. Diodes were missed in the original order. Some larger small-outline-diodes (SOD) 123 were used instead of the originally specified (SOD 523) components. This required some creative component soldering.
4. AD cross-schematic labelling: Two label errors in the schematics resulted in crossed lines on the PCB. To correct these, several resistors were rotated out of their normal silkscreen placement positions. The resistors were cross connected using short pieces of Kynar wire.
5. The 100 kΩ load resistor was not included in the final PCB. To correct this, a through-hole component was soldered from the signal header pin to the ground header pin.
6. Two failed 10 kΩ resistors were identified, both within two of the thirteen-resistor-long (series) voltage-divider spines. By consequence, no current flowed and the voltage thresholds were incorrect. The components were identified and replaced.
7. Operational amplifier configuration: Four operational amplifier chips (sixteen operational amplifiers in total) were wired in reverse for input and output. This was corrected by sitting the chips "dead bug" (upside-down) and rerouting connections.
8. Introduced noise: Likely stemming from the circuit corrections and Kynar wire, significant noise was present in many of the signals. Most of the noise across all stages could be reduced by implementing additional, larger, bypass capacitors. The output was not able to be corrected within the project timeframe remaining post-fabrication.

## 5.2.0 System Testing

To test the board, 3.3 V supply with a 1 A limiter was applied. Typically, the voltage received by the board varied in the range of 3.25 V ~ 3.35 V as the supply was set higher than 3.3 V due to a voltage drop in the power cable (as the current varied in the range of 700 – 900 mA). An oscilloscope was used to probe various outputs; several of these have been included in the following figures.


Figure 5.2.0A: Input circuit. The initial sawtooth (yellow) is offset by a voltage subtraction (purple), before a gain stage (blue). This process is repeated to construct the final waveform (green) which should vary from 0 to 3.3 V. This sawtooth is the master control signal. This signal is buffered before reception at the tile group control block. Some safety room was inbuilt into the signal; despite the amplitude not reaching 3.3 V, there is sufficient amplitude for full system function.




Figure 5.2.0B: The post-buffer control signal. Some noise is present on the sawtooth, corresponding to switch points for each tile control group. This noise varies significantly in position and intensity over operation; in this image, the noise is most intense in the Tile 2 boundary (second-bottom quarter of the sawtooth).

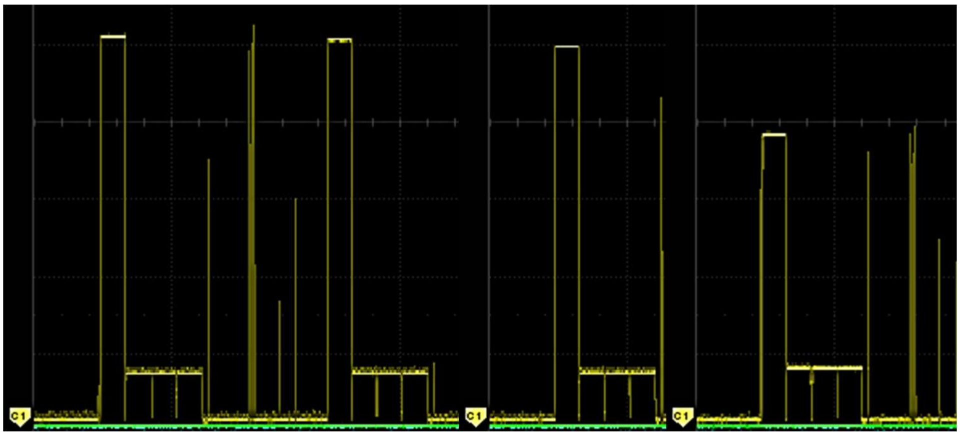

Figure 5.2.0G: A single plate set pulse, with amplitude varying due to plate set health. This signal is prior to the summation (with other plate sets on a tile) and the offset, gain stages that improve threshold distinction. Spikes of noise present correspond to those visible and discussed in Figure 5.2.0D.

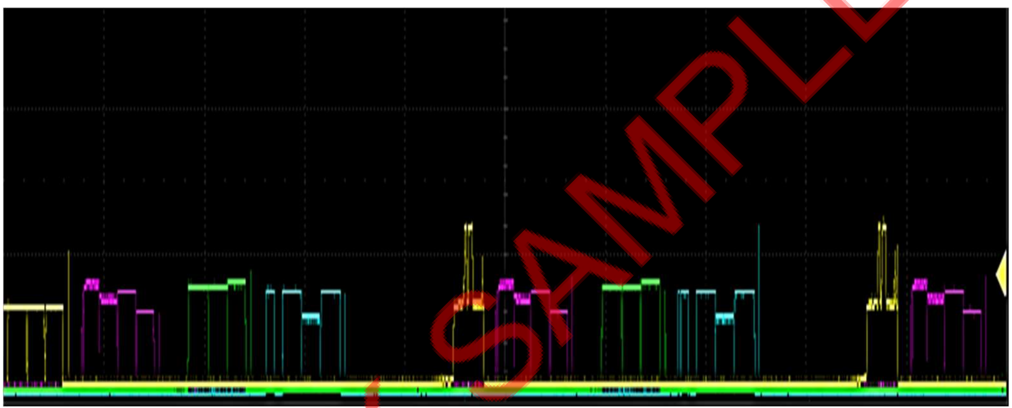

Figure 5.2.0H: Cropped, zoomed, enhanced image of all tile outputs. Significantly less noise is present than in the final output. As is evident, over the two-and-a-quarter periods sampled, the first tile output is typically much noisier than the other tiles. Tile group two is consistently correct, with all pulses present and same width. This agrees with the behaviour observed in Figure 5.2.0C (probe colours correspond between figures for reference).

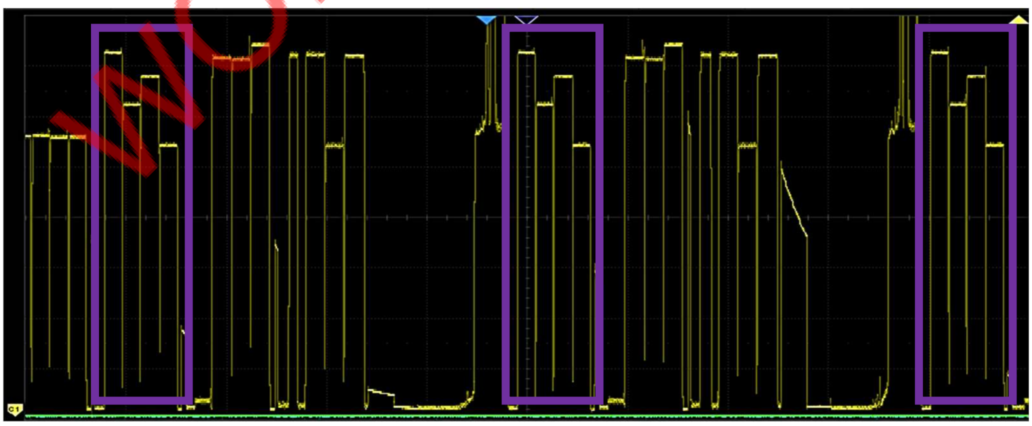

Figure 5.2.0I: System output with various configurations of tile health. The period can be seen repeating roughly two-and-a-quarter times; the start of a new period is indicated by the absence of any pulse for a time corresponding to a tile's information. The first period shown is much less noisy than the latter two. The second tile, highlighted by the purple box, can be consistently shown to produce a clean signal. This indicates strong proof of concept; with noise reduction, the system should function as theorised.

# 6.0.0 Conclusion

As was observed in system testing (Section 5.2.0) the anticipated system behaviour that was modelled in 3.0.0 and simulated in 4.0.0 has been achieved. Noise is present in the signals however this is likely due to corrections that had to be made to the PCB due to fabrication issues. On the noise-free tile, the tile state is clearly defined with measurable and comparable thresholds.

As the tile group has been successfully validated, the next step would be to implement several tile groups and the controller module. The recommendation for this stage would be to produce separate PCBs for each module, which will aid in production and testing of the system. Furthermore, the introduction of additional surface mount capacitor pads would aid in mounting bypass capacitors. For diagnosing issues, some solderable bridges on key traces would prove useful (as by de-soldering these, blocks of the system can be isolated and analysed independently). For probing, some probe loop components at all key signal points would aid in producing results; as with any system that requires more than two probes for inter-system comparison, manoeuvring multiple probes becomes extremely tedious especially with surface mount components.

This thesis discusses and demonstrates the model, however the physical application to space structures has not been readily investigated. An investigation into the feasibility of a multi-layer system for three-dimensional impact detection, building upon the system described, could result in a superior system.

On foundation of this thesis, the initial aims were as follows (as per Section 3.0.0):

1. **To create a Prototype:** This has been achieved with an end-to-end system. Despite the scope reduction from multiple tile groups and a controller to a singular tile group, the project outcome has succeeded in providing a solution to the niche identified.
2. **Component Selection:** The tile group cost was approximately $900 AUD. This was in excess of the intended budget (sub $500 AUD), however many factors contributed. The most significant was that of the current global silicon shortage and supply issues with ICs, which drove the price up significantly. Mass production after tuning would result in an inexpensive product.
3. **Target Destination:** The system is lightweight and entirely analogue. This is ideal for space.
4. **Competitive:** No microcontrollers are required. Power consumption is currently high however this is expected, as the prototype built has not have the appropriate ratio of control blocks to plate sets and plates. On a real application, the power consumption would likely be admirable.
5. **Implementation:** The system is extremely flexible and shows promise for integration in new and existing structures for both 2D and 3D mechanical deformation detection.
6. **Maintenance and Longevity:** The system is modular and consists entirely of analogue and passive components, for which there is an unending global supply over the lifetime of electronics as an engineering application.

Therefore, it can be said the thesis has achieved all goals set.

Owen Claxton
Prof. Clinton Fookes
Assoc. Prof. Luis Mejias Alvarez
Dr. Jonathon Ralston

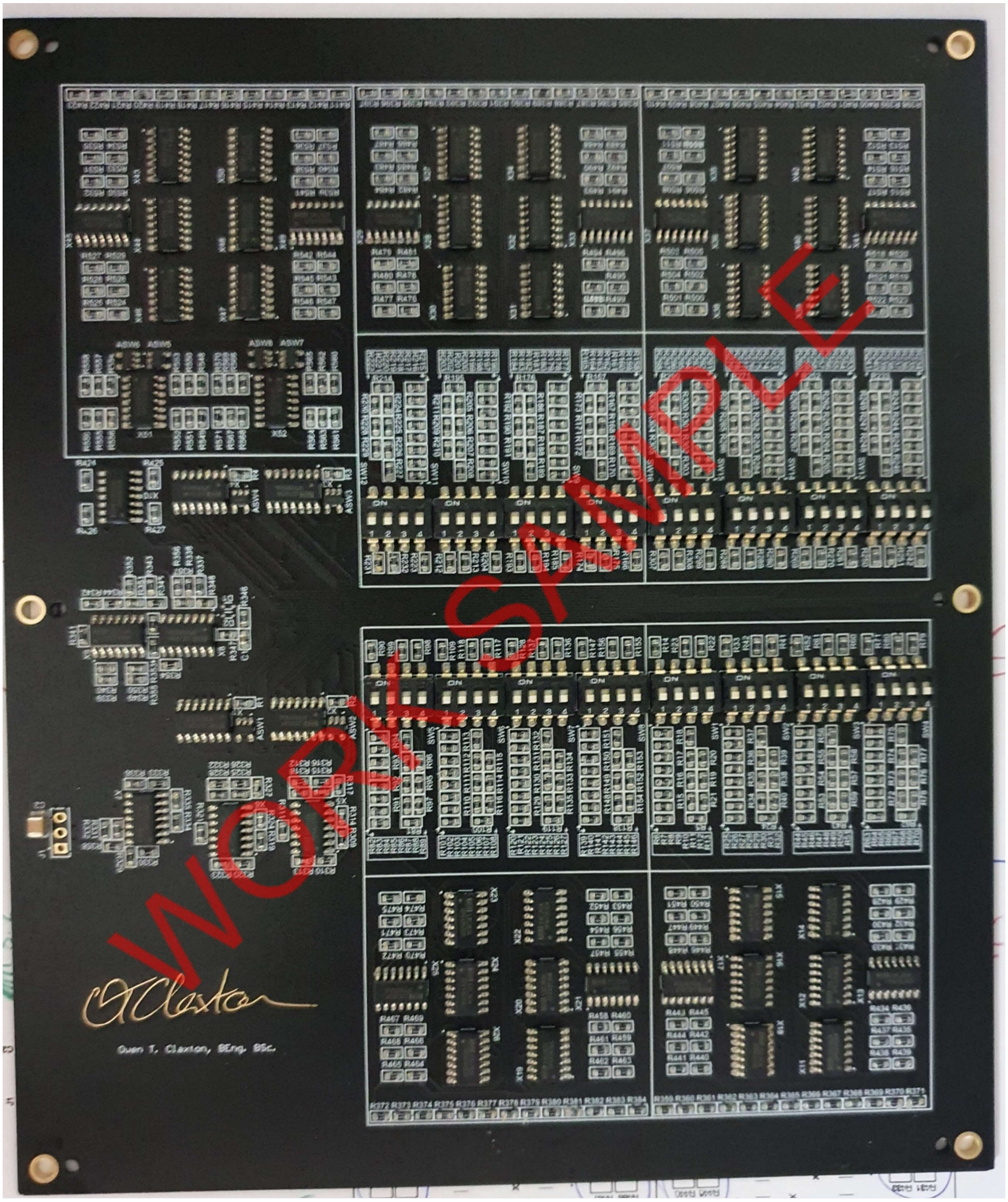


Figure C.1D: Full board, post component placement (pre-reflow of upper surface).

Owen Claxton
Prof. Clinton Fookes
Assoc. Prof. Luis Mejias Alvarez
Dr. Jonathon Ralston

# Appendix G – Altium Schematics

Note: Only a single example control and plate set schematic have been provided (for Tile 1).

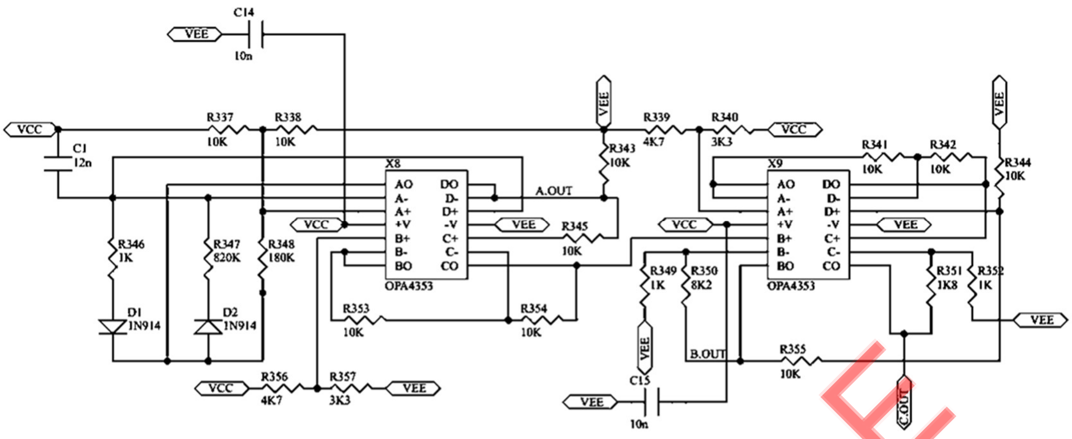

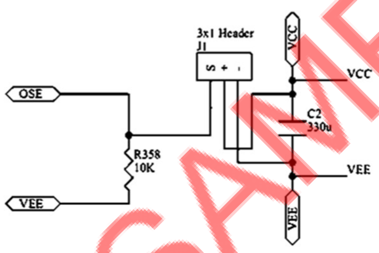

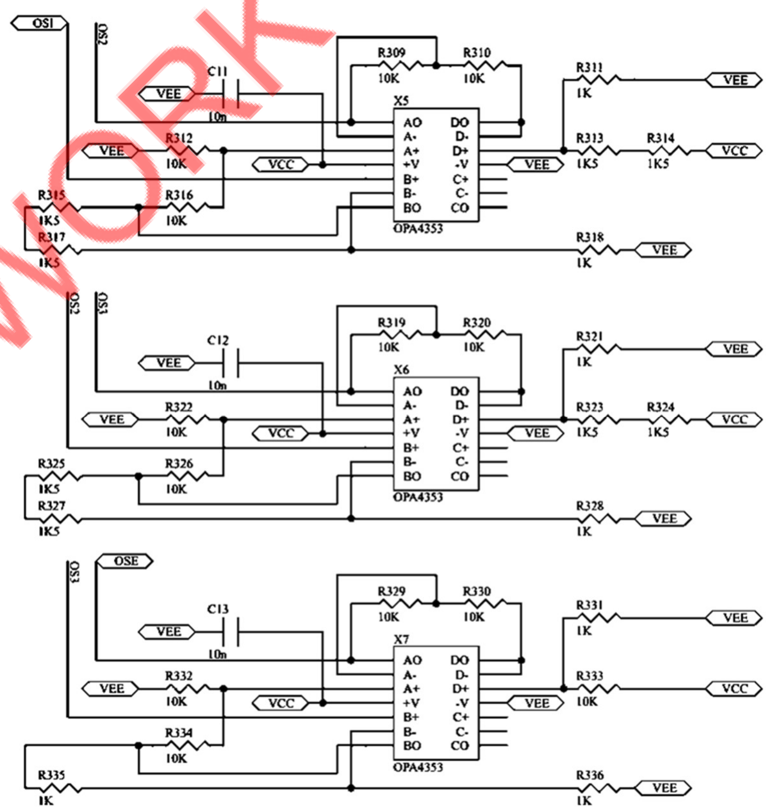

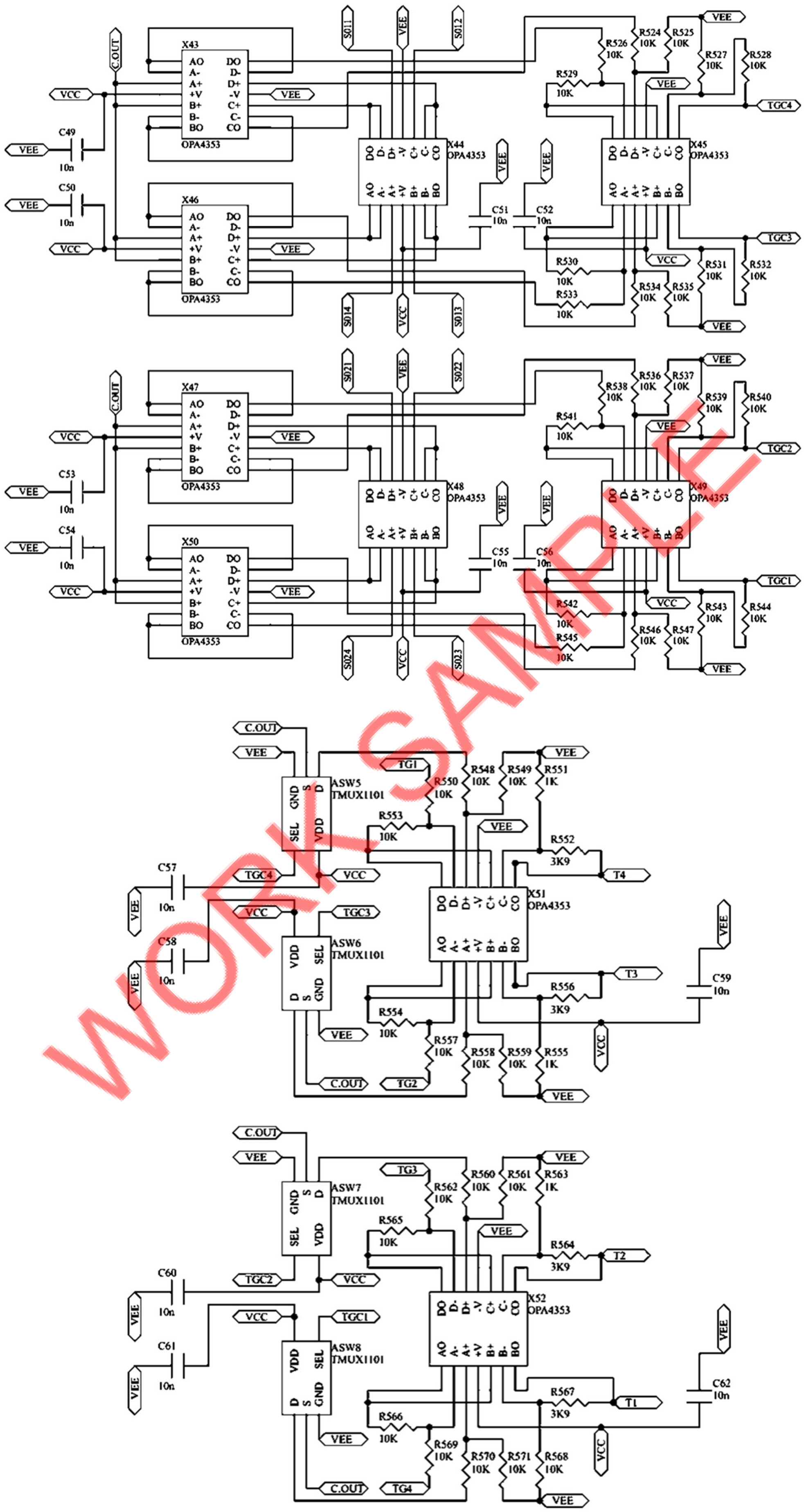
X43
OPA4353
X44
OPA4353
X45
OPA4353
X46
OPA4353
X47
OPA4353
X48
OPA4353
X49
OPA4353
X50
OPA4353
X51
OPA4353
X52
OPA4353
ASW5
TMUX1101
ASW6
TMUX1101
ASW7
TMUX1101
ASW8
TMUX1101
C.OUT
VCC
VEE
TGC1
TGC2
TGC3
TGC4
TG1
TG2
TG3
TG4
T1
T2
T3
T4
SO11
SO12
SO13
SO14
SO21
SO22
SO23
SO24

Owen Claxton
Prof. Clinton Fookes
Assoc. Prof. Luis Mejias Alvarez
Dr. Jonathon Ralston

## G.1.2 Project Timeline

### EGH400 Timeline

| Semester | Type | Title | ID | Planned Start | Planned Duration | Actual Start | Actual Duration | Percent Complete |
|---|---|---|---|---|---|---|---|---|
| 1 | Management & Communication | Update Emails | M.1 | 1 | 16 | 1 | 16 | 100% |
| 1 | | Virtual Meetings | M.2 | 9 | 8 | 9 | 8 | 100% |
| 2 | | Update Emails | M.3 | 22 | 15 | 22 | 17 | 100% |
| 2 | | Virtual Meetings | M.4 | 22 | 15 | 22 | 17 | 100% |
| 1 | Key University Periods | Mid Semester Break | K.1 | 6 | 1 | 6 | 1 | 100% |
| 1 | | Exam Block | K.2 | 15 | 2 | 15 | 2 | 100% |
| - | | Mid Year Break | K.3 | 17 | 5 | 17 | 5 | 100% |
| 2 | | Mid Semester Break | K.4 | 31 | 1 | 31 | 1 | 100% |
| 2 | | Exam Block | K.5 | 36 | 1 | 36 | 1 | 100% |
| 1 | Assessment Schedule | Obtain a Project | A.1 | 1 | 2 | 1 | 2 | 100% |
| 1 | | Assessment 1A | A.2 | 3 | 1 | 3 | 1 | 100% |
| 1 | | Assessment 1B | A.3 | 8 | 1 | 8 | 1 | 100% |
| 1 | | Assessment 2A | A.4 | 15 | 1 | 15 | 1 | 100% |
| 1 | | Assessment 2B | A.5 | 15 | 1 | 18 | 1 | 100% |
| 2 | | Assessment 1 | A.6 | 28 | 1 | 26 | 1 | 100% |
| 2 | | Assessment 2A | A.7 | 36 | 1 | 36 | 1 | 100% |
| 2 | | Assessment 2B | A.8 | 36 | 1 | 36 | 1 | 100% |
| 2 | | Assessment 3 | A.8 | 36 | 1 | 38 | 1 | 100% |
| 1 | Stages & Milestones | Milestone 1 | S.1 | 8 | 1 | 8 | 1 | 100% |
| 1 | | Milestone 2 | S.2 | 15 | 1 | 15 | 1 | 100% |
| 2 | | Milestone 3 | S.3 | 22 | 1 | 22 | 1 | 100% |
| 2 | | Milestone 4 | S.4 | 28 | 1 | 28 | 1 | 100% |
| 2 | | Milestone 5 | S.5 | 36 | 1 | 38 | 1 | 100% |
| 1 | Stage 1: Project Initialisation | Project Overview | P1.1 | 1 | 2 | 1 | 2 | 100% |
| 1 | | Client and Relevancy | P1.2 | 2 | 2 | 3 | 2 | 100% |
| 1 | | Considerations & Limitations | P1.3 | 2 | 2 | 3 | 1 | 100% |
| 1 | | Literature Review & Discussion | P1.4 | 2 | 5 | 2 | 7 | 100% |
| 1 | | Milestones & Deliverables | P1.5 | 3 | 2 | 5 | 4 | 100% |
| 1 | | Communication Plan | P1.6 | 3 | 2 | 6 | 3 | 100% |
| 1 | Stage 2: Focussed Research & Ideation | Supporting Research | P2.1 | 9 | 7 | 9 | 7 | 100% |
| 1 | | Progress Updates | P2.2 | 14 | 2 | 15 | 1 | 100% |
| 1 | | Risk Identification & Assessment | P2.3 | 10 | 1 | 15 | 1 | 100% |
| 1 | | Sustainability Statements & Review | P2.4 | 11 | 1 | 15 | 1 | 100% |
| 1 | | Ethics Statements & Review | P2.5 | 11 | 1 | 15 | 1 | 100% |
| 1 | | Ideation | P2.6 | 10 | 6 | 9 | 7 | 100% |
| 1 | | Initial Designs | P2.7 | 14 | 2 | 10 | 6 | 100% |
| 1 | Stage 3: Selection of Design | Detailed Initial Design Production | P3.1 | 16 | 7 | 12 | 2 | 100% |
| 1 | | Design Assessment | P3.2 | 16 | 7 | 13 | 2 | 100% |
| 2 | | Design Selection and Next Steps | P3.3 | 16 | 7 | 15 | 4 | 100% |
| 2 | Stage 4: Detailed Design Process | LTspice Circuit Construction | P4.1 | 17 | 12 | 17 | 12 | 100% |
| 2 | | Board Design | P4.2 | 25 | 2 | 25 | 3 | 100% |
| 2 | | Parts Ordering | P4.3 | 26 | 2 | 35 | 4 | 100% |
| 2 | | Board Fabrication | P4.4 | 27 | 2 | 32 | 1 | 100% |
| 2 | Stage 5: Production & Testing of Design | Design Production | P5.1 | 29 | 6 | 36 | 2 | 100% |
| 2 | | Design Testing | P5.2 | 32 | 3 | 36 | 2 | 100% |
| 2 | | Review of Results | P5.3 | 34 | 2 | 36 | 2 | 100% |
| 2 | | Final Document Production | P5.4 | 29 | 8 | 36 | 3 | 100% |

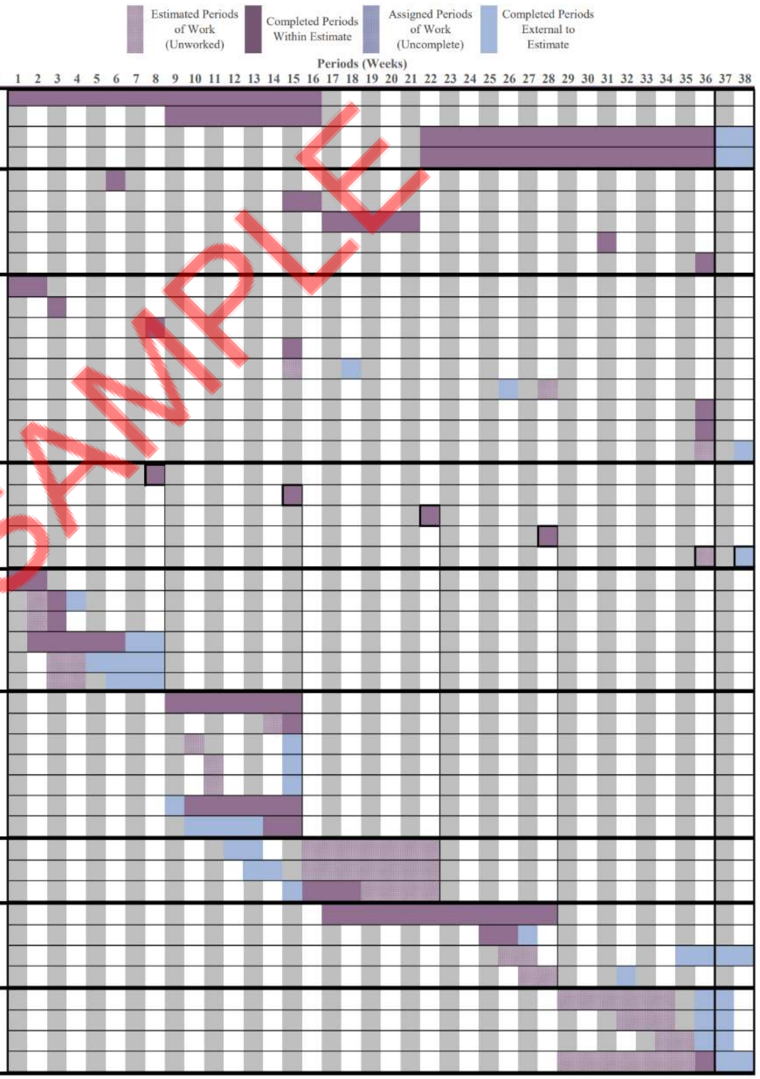


Figure G.1.2A: Gantt chart depicting the EGH400 Timeline for 2021. Due to nan extension, the original final submission date was extended.